

Temporal Effective Medium for Programmable Acoustic Metamaterials with Multiple Resonances

Xinghong Zhu¹, Hong-Wei Wu^{3*}, and Jensen Li^{1,2*}

¹Department of Physics, The Hong Kong University of Science and Technology, Clear Water Bay, Hong Kong, China

²Department of Engineering, University of Exeter, EX4 4QF, United Kingdom

³School of Mechanics and Photoelectric Physics, Anhui University of Science and Technology, Huainan 232001, China

We extend effective medium theory (EMT) to time-modulated, frequency-dispersive acoustic metamaterials with multiple resonances. While previous studies focused on non-dispersive or single-resonance systems, advances in programmable materials now enable precise control of time-varying responses. We derive explicit averaging rules that account for the interplay between resonant and modulation frequencies. When resonant frequencies are much lower than the modulation frequency, modulating the resonant strength yields the temporal average of monopolar susceptibility χ , while modulating the resonant frequency results in the average of $1/\chi$, applied per resonance mode. In hybrid cases, high-frequency resonances (relative to modulation) can be renormalized as a non-dispersive background before averaging the rest. This generalized temporal EMT offers a unified framework for designing compact, topologically robust, and non-Hermitian acoustic devices, leveraging the possible programmability of time-dependent material parameters in future.

* Emails: j.li13@exeter.ac.uk; hwwu@aust.edu.cn

INTRODUCTION

Metamaterials, built from periodic meta-atoms, have enabled unprecedented wave manipulation, including negative refraction, superlensing, and perfect absorption [1-4]. A key concept is the use of effective medium theory (EMT) [5-12], which describes subwavelength structures using macroscopic parameters. EMT supports a two-step design process: first, defining the desired effective medium profile; then, engineering the metamaterial to realize it by either numerical effective medium extraction or formulas. This approach has enabled many exotic wave phenomena including invisibility cloak, super resolution imaging, wave tunneling, amplification, sensing and beyond [13-19]. Recently metamaterials have been extended to the time-varying regime, where time-varying material parameters are used as a new degree of freedom for wave control. Time-varying metamaterials enable four-dimensional modulation (x, y, z, t) [20-22], giving rise to effects like temporal refraction, frequency conversion, nonreciprocity, and momentum bandgaps [23-39]. These developments have spurred extensions of EMT into the temporal domain, typically requiring modulation frequencies much higher than the signal frequency. Existing formulations, however, mostly address non-dispersive or single-resonance systems [40-43].

A promising route for a fast temporal modulation in acoustics uses meta-atoms with digital feedback circuits, enabling real-time tunability [29,44]. This method also supports modulation of generalized resonance types. Similar to how complex electromagnetic dispersion can be modeled by multiple Lorentzian resonances, digital feedback allows analogous implementations in time-varying systems. Although single-resonance temporal EMT has been experimentally demonstrated [45,46], a general framework for multi-resonance systems remains undeveloped.

In this work, we extend the temporal effective medium theory to encompass frequency-dispersive metamaterials with multiple resonances, focusing on acoustic systems for clarity and demonstration. By modulating different resonance parameters, such as resonant frequency and strength, we derive effective medium formulas that account for the interplay between resonant frequencies and modulation frequency. Our results reveal that when resonant frequencies are much smaller than the modulation frequency, modulating resonant strength follows temporal averaging of monopolar susceptibility directly, while modulating

resonant frequency inverts this relationship, producing reciprocal averaging, applied separately to each resonance mode. These principles enable precise control over effective responses, even in hybrid regimes where some resonant frequencies fall in the non-dispersive regime (much higher than the modulation frequency), these modes will suppress dispersion in their resonances, forming an effectively static, renormalized background. This allows the dispersive component to be time-averaged with the normalized background. These findings provide a critical foundation for understanding and designing temporal metamaterials with fast modulation, enabling compact, topologically robust, and non-Hermitian acoustic devices with tailored functionalities achievable through time-varying material parameters in future. Furthermore, the principles developed here can be extended to other wave systems, opening new possibilities for programmable metamaterial design.

RESULTS

Modulating resonant strength with two resonances

We begin with a one-dimensional (1D) spatially homogeneous acoustic medium along x , where the material properties are modulated in time t to generate monopolar polarization $M(x, t)$ in the surrounding air. The acoustic wave propagation in this medium is governed by the following equations:

$$\partial_x p(x, t) + \rho_0 \partial_t v(x, t) = 0, \quad (1)$$

$$\partial_x v(x, t) + \beta_0 \partial_t (p(x, t) + M(x, t)) = 0, \quad (2)$$

where ρ_0 and β_0 are the density and compressibility of air, and $p(x, t)$ and $v(x, t)$ are the pressure and velocity fields, respectively. We assume the metamaterial possesses only monopolar responses, composed of several resonant modes by $M(x, t) = \sum_i M_i(x, t)$ and generate monopolar susceptibility $\chi = \sum_i \chi_i$. Each monopolar response $M_i(x, t)$ corresponds to the i -th resonant mode and interacts with the pressure field $p(x, t)$ according to a Lorentzian-type model:

$$\partial_t^2 M_i(x, t) + 2\gamma_i(t) \partial_t M_i(x, t) + \omega_{0i}^2(t) M_i(x, t) = a_i(t) p(x, t), \quad (3)$$

where $a_i(t)$, $\omega_{0i}(t)$ and $\gamma_i(t)$ the time-dependent resonant strength (with units of squared frequency), resonant frequency, and linewidth of the i -th resonance, respectively. As shown in

Fig. 1(a), the three resonance parameters $(a_i, \omega_{0i}, \gamma_i)$ are modulated periodically with period T , consisting of two phases. Phase A lasts for ξT (duty cycle ξ), during which the parameters remain constant as $(a_{iA}, \omega_{0iA}, \gamma_{iA})$. Phase B spans the remaining $(1 - \xi)T$ with parameters $(a_{iB}, \omega_{0iB}, \gamma_{iB})$. For clarity, we focus on monopolar polarizations with two resonances ($i = 1, 2$), while cases with more resonances can be derived from the findings for two resonances. Figure 1(b) schematically depicts the static compressibility β_A and β_B ($\beta = 1 + \chi_1 + \chi_2$), each featuring two resonances in phases A and B, assuming no time modulation. Our goal is to derive the temporal effective medium formula for modulating these phases with duty cycle ξ in terms of β_A and β_B . The formulas vary significantly depending on which resonance parameters (e.g., strength or resonant frequency) or their combinations are modulated, and whether the non-dispersive limit is approached by having the resonant frequency ω_0 much larger than the modulation frequency $1/T$.

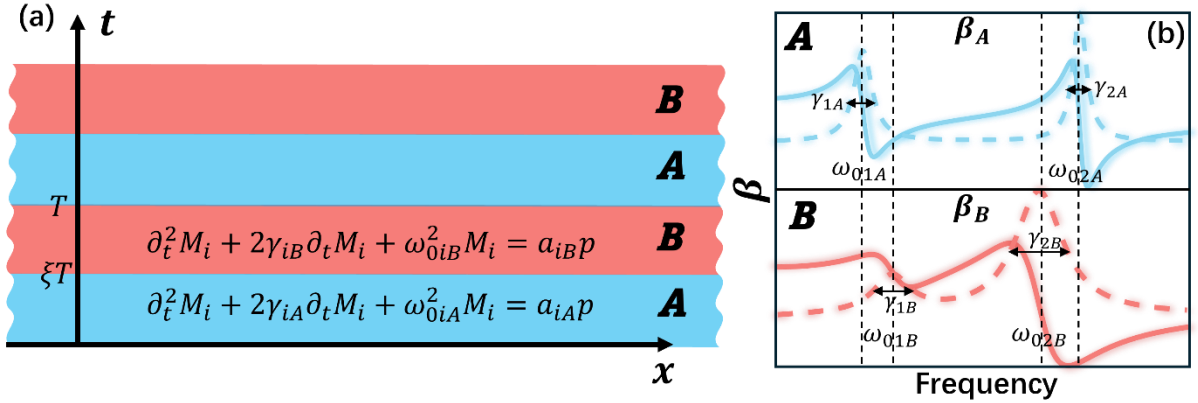


Fig. 1 Schematic diagram of a time-varying metamaterial with multiple resonance modes. (a) Each resonance i has a monopolar polarization M_i driven by pressure p , governed by Lorentzian-type differential equations with resonant frequency, strength and linewidth switching phases A and B, with modulation period T and duty cycle $\xi: 1 - \xi$. (b) Static effective compressibility β_A and β_B in phases A (blue) and B (red), assuming no time modulation, with $\omega_{0iA}, \omega_{0iB}$ and γ_{iA}, γ_{iB} as the resonant frequencies and linewidths for resonance i , respectively. Solid (dashed) lines represent the real (imaginary) parts.

Firstly, we consider the case where only the resonant strengths $a_1(t)$ and $a_2(t)$ are time modulated, while the other parameters ω_{0i} and γ_i remain constant, as shown in Fig. 2(a). To derive the temporal effective medium, we assume the medium is homogenous and infinite along the x direction, ensuring that the propagation constant k remains unchanged across

different time interfaces. Substituting ∂_x with ik , Eq. (1)-(3) can be rewritten as

$$i\partial_t\psi = \hat{\omega}\psi, \quad \hat{\omega} = \begin{pmatrix} 0 & k/\beta_0 & 0 & i & 0 & i \\ k/\rho_0 & 0 & 0 & 0 & 0 & 0 \\ 0 & 0 & 0 & -i & 0 & 0 \\ -ia_1(t) & 0 & i\omega_{01}^2 & -2i\gamma_1 & 0 & 0 \\ 0 & 0 & 0 & 0 & 0 & -i \\ -ia_2(t) & 0 & 0 & 0 & i\omega_{02}^2 & -2i\gamma_2 \end{pmatrix}, \quad (4)$$

with the eigenstate vector $\psi = (p, v, M_1, -\partial_t M_1, M_2, -\partial_t M_2)^T$. The propagation matrix $\hat{\omega}$, alternates between $\hat{\omega}_A$ and $\hat{\omega}_B$, corresponding to resonant strength a_{1A} , a_{2A} and a_{1B} , a_{2B} respectively. In the two static cases, Eq. (1)-(3) can be solved time-harmonically and combined with the constitutive relationship $p + M = \beta p = (1 + \chi_1 + \chi_2)p$ with $M = M_1 + M_2$, where β is the effective compressibility and χ_i is the effective susceptibility relative to air for the i -th resonance. This yields

$$\beta_{A/B} = 1 + \chi_{1A/B} + \chi_{2A/B} = 1 + \frac{a_{1A/B}}{\omega_{01}^2 - \omega^2 - 2i\omega\gamma_1} + \frac{a_{2A/B}}{\omega_{02}^2 - \omega^2 - 2i\omega\gamma_2}. \quad (5)$$

An example of the compressibility for two static phases is shown in Fig. 2(b), with blue and red lines representing phases A and B, respectively, and solid/dashed lines indicating the real/imaginary parts. For phase A (blue), the resonant frequencies are set as $\omega_{01}/(2\pi) = 1\text{kHz}$, $\omega_{02}/(2\pi) = 1.5\text{kHz}$, with linewidths $\gamma_1/\omega_{01} = \gamma_2/\omega_{02} = 0.05$. The resonant strengths are $a_{1A}/\omega_{01}^2 = a_{2A}/\omega_{02}^2 = 0.2$. In phase B (red), the resonant strengths change to $a_{1B}/\omega_{01}^2 = 0.5$ and $a_{2B}/\omega_{02}^2 = 0.6$, while all other parameters remain constant. In the time-varying case, the resonant strengths switch between a_{iA} and a_{iB} . Assuming the modulation period T satisfies $\omega T \ll 1$ and $\omega_{0i}T \ll 1$, the modulation frequency is much higher than both the signal frequency (or eigenfrequency in the medium) and the resonant frequencies. Under these conditions, the total transfer matrix $\exp(-i\hat{\omega}_B(1-\xi)T)\exp(-i\hat{\omega}_AT)$ can be approximated as $\exp(-i\hat{\omega}_{\text{eff}}T)$, where $\hat{\omega}_{\text{eff}} = \xi\hat{\omega}_A + (1-\xi)\hat{\omega}_B$ in the first order Taylor expansion of T . Using Eq. (5), the effective compressibility for modulating a_i is given by

$$\beta_{\text{eff}} = 1 + \chi_{1\text{eff}} + \chi_{2\text{eff}}. \quad (6)$$

$$\chi_{1\text{eff}} = \xi\chi_{1A} + (1-\xi)\chi_{1B}, \quad \chi_{2\text{eff}} = \xi\chi_{2A} + (1-\xi)\chi_{2B}. \quad (7)$$

The result corresponds to the temporal average of compressibility β or, equivalently, the susceptibility χ .

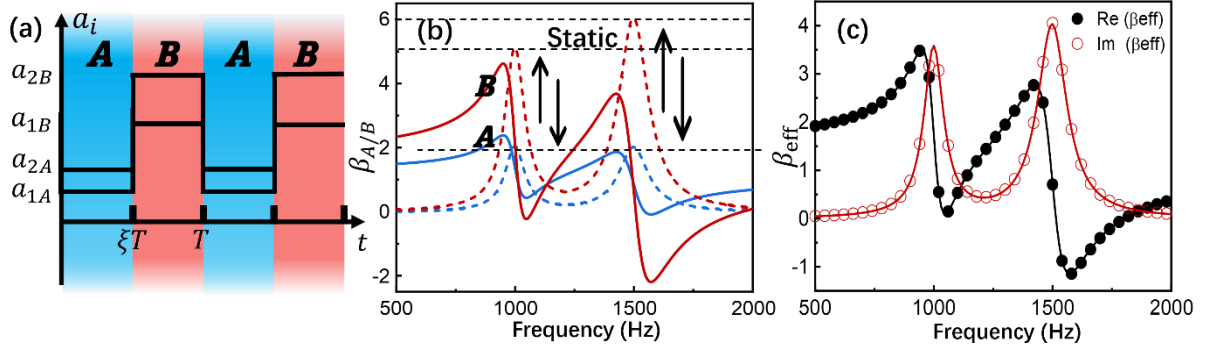


Fig. 2 (a) Sketch of time-varying metamaterials with two monopolar resonant strengths modulated over period T and duty cycle ξ . (b) Static compressibility β_A (blue) in phase A and β_B (red) in phase B, with solid (dashed) line representing real (imaginary) parts. The parameters are chosen as $\omega_{01}/(2\pi) = 1$ kHz, $\omega_{02}/(2\pi) = 1.5$ kHz, $a_{1A}/\omega_{01}^2 = a_{2A}/\omega_{02}^2 = 0.2$, $a_{1B}/\omega_{01}^2 = 0.5$, $a_{2B}/\omega_{02}^2 = 0.6$, $\gamma_1/\omega_{01} = \gamma_2/\omega_{02} = 0.05$. (c) Effective compressibility β_{eff} extracted using the eigenmode approach (red and black dots), with $a_1(t)$ switching between a_{1A} and a_{1B} and $a_2(t)$ switching between a_{2A} and a_{2B} ($\xi = 0.5$). Analytic results (red and black lines) are from Eq. (6) and (7). Modulation frequency: $1/T = 8$ kHz; other parameters as in (b).

Alternatively, the eigenmode of Eq.(4) can be numerically solved using the transfer matrix method. At a small eigenfrequency ω , we can extract the effective compressibility β_{eff} and density ρ_{eff} (relative to air) from the eigenstate as [46]

$$\beta_{\text{eff}} = \frac{k}{\omega \rho_0} \frac{p + M}{v}, \quad (8)$$

$$\rho_{\text{eff}} = \frac{k}{\omega \beta_0} \frac{v}{p + M}.$$

This approach is employed to generate all numerical results in the following. As an example, we modulate resonant strength $a_i(t)$ with the modulation parameters used in Fig. 2(b) with duty cycle $\xi = 0.5$ and calculated the effective compressibility β_{eff} marked as black and red hollow dots for real and imaginary part against operational frequency $\omega/(2\pi)$ in Fig. 2(c). These results match well with the effective formula of time averaging χ_i for each mode by Eq.(7) and thus obtaining the effective compressibility by Eq. (6), as plot in black and red lines.

Modulating resonant frequency with two resonances

Following the case of modulating resonant strength a_i , we now consider modulating resonant frequency ω_{0i} while keeping a_i and γ_i constant, as shown in Fig. 3(a). ω_{0i} switches between ω_{0iA} and ω_{0iB} in phases A and B, respectively. We still require $\omega_{0iA/B}T \ll 1$ in both phases. This allows us to approximate the effective propagation matrix using the lowest-order Talor expansion: $\hat{\omega}_{\text{eff}} = \xi \hat{\omega}_A + (1 - \xi) \hat{\omega}_B$. The temporal effective medium formula in modulating ω_{0i} can then be expressed in terms of the static susceptibilities as

$$1/\chi_{1\text{eff}} = \xi/\chi_{1A} + (1 - \xi)/\chi_{1B}, \quad 1/\chi_{2\text{eff}} = \xi/\chi_{2A} + (1 - \xi)1/\chi_{2B}, \quad (9)$$

where the static monopolar susceptibility in each phase is

$$\chi_{1A/B} = \frac{a_1}{\omega_{01A/B}^2 - \omega^2 - 2i\omega\gamma_1}, \quad \chi_{2A/B} = \frac{a_2}{\omega_{02A/B}^2 - \omega^2 - 2i\omega\gamma_2}. \quad (10)$$

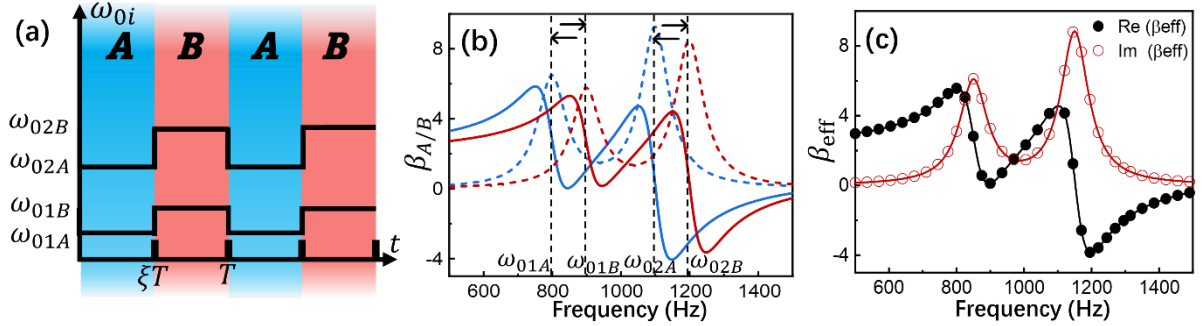


Fig. 3 Time-varying metamaterial with modulated resonant frequencies. (a) Schematic diagram of metamaterial with resonant frequency ω_{0i} switching between ω_{0iA} and ω_{0iB} . (b) Static compressibility in phase A (blue) with $\omega_{01A}/(2\pi) = 0.8$ kHz, $\omega_{02A}/(2\pi) = 1.1$ kHz and in phase B (red) with $\omega_{01B}/(2\pi) = 0.9$ kHz, $\omega_{02B}/(2\pi) = 1.2$ kHz. (c) Effective compressibility when modulating resonant frequency according to (b) with duty cycle $\xi = 0.5$, with dots from the eigenmode approach (Eq. (8)) and lines from Eq. (9). The resonant strength and linewidth are both constants: $a_1/(2\pi)^2 = 0.5$ kHz², $a_2/(2\pi)^2 = 1$ kHz², $\gamma_1/(2\pi) = \gamma_2/(2\pi) = 50$ Hz.

Figure 3(b) shows the static compressibility for phase A (blue) and phase B (red) as a function of operational frequency $\omega/(2\pi)$, with solid and dashed lines representing real and imaginary parts, respectively. The resonant frequencies are $\omega_{01A}/(2\pi) = 0.8$ kHz and $\omega_{02A}/(2\pi) = 1.1$ kHz for phase A, and $\omega_{01B}/(2\pi) = 0.9$ kHz and $\omega_{02B}/(2\pi) = 1.2$ kHz for phase B. The resonant strengths and linewidths remain constant: $a_1/(2\pi)^2 = 0.5$ kHz², $a_2/(2\pi)^2 = 1$ kHz², $\gamma_1/(2\pi) = \gamma_2/(2\pi) = 50$ Hz. After defining the static compressibilities for the two phases, they are alternated with a duty cycle of $\xi = 0.5$. The effective

compressibility β_{eff} is calculated using the eigenmode approach and shown in Figure 3(c) as black and red hollow dots for the real and imaginary parts. These results align with the analytic predictions (solid lines) obtained from Eq. (9), confirming the accuracy of the time-averaging approach for $1/\chi_i$.

Effective medium formulas with $\omega_{01}T \ll 1$ and $\omega_{02}T \gg 1$

Thus far, we have presented modulation cases satisfying both $\omega T \ll 1$ and $\omega_{0i}T \ll 1$. While $\omega T \ll 1$ is a necessary condition for the temporal effective medium criteria, $\omega_{0i}T \ll 1$ is not. When both resonant frequencies ω_{01} and ω_{02} are sufficiently large ($\omega_{0i}T \gg 1$), the system approaches the so-called frequency-nondispersive regime. In this case, modulating a_i allows the susceptibilities to be expressed as $\chi_{1A/B} = a_{1A/B}/\omega_{01}^2$ and $\chi_{2A/B} = a_{2A/B}/\omega_{02}^2$ with a_i scaling with ω_0^2 to have non-zero χ_i . Although $\omega T \ll 1$ still holds, the large $\omega_{0i}T$ prevents the direct application of the first-order Taylor expansion. However, if the resonant linewidth γ_i is sufficiently large, it can suppress the rapid oscillation of monopolar polarization M_i triggered at each time boundary and approach the new static regime. By examining Eq. (4) for large ω_{0i} , the wave equation in phase A/B can be approximated as

$$i\partial_t(p + M) \cong \frac{k}{\beta_0} v, \quad i\partial_t v \cong \frac{k}{\rho_0} \frac{1}{1 + \chi_{1A/B} + \chi_{2A/B}} (p + M), \quad (11)$$

which effectively reduces the propagation matrix $\hat{\omega}$ in Eq. (4) from 6×6 to 2×2 and yields the temporal effective formula for time-varying modulation amplitude $a_i(t)$ at large ω_{0i} :

$$\frac{1}{1 + \chi_{1\text{eff}} + \chi_{2\text{eff}}} = \frac{\xi}{1 + \chi_{1A} + \chi_{2A}} + \frac{1 - \xi}{1 + \chi_{1B} + \chi_{2B}}. \quad (12)$$

This result ($\beta_{\text{eff}} = 1 + \chi_{1\text{eff}} + \chi_{2\text{eff}}$) corresponds to the temporal average of $1/\beta$, as first investigated by Engheta [41] for non-dispersive time-varying media.

After recognizing that effective medium formulas can be influenced by the value of ω_{0i} , we consider a hybrid case where $\omega_{01}T \ll 1$ and $\omega_{02}T \gg 1$. Under this condition, only $\chi_{2A/B}$ can be expressed as $\chi_{2A/B} = a_{2A/B}/\omega_{02}^2$ through modulation of a_i . Together with Eqs. (1)-(3), the original 6×6 eigenvalue problem (Eq. (4)) can be truncated to a 4×4 system:

$$i\partial_t\psi = \hat{\omega}\psi, \quad \hat{\omega} = \begin{pmatrix} 0 & k/\beta_0 & 0 & i \\ \frac{k/\rho_0}{1+\chi_2(t)} & 0 & 0 & 0 \\ 0 & 0 & 0 & -i \\ -\frac{ia_1(t)}{1+\chi_2(t)} & 0 & i\omega_{01}^2 & -2i\gamma_1 \end{pmatrix}, \quad (13)$$

where now the state vector becomes $\psi = (p + M_2, v, M_1, -\partial_t M_1)^T$. The propagation matrix $\hat{\omega}_A$ and $\hat{\omega}_B$ correspond to the parameter pairs (a_{1A}, χ_{2A}) and (a_{1B}, χ_{2B}) , respectively. The total transfer matrix $\exp(-i\hat{\omega}_B(1-\xi)T)\exp(-i\hat{\omega}_AT)$ can be approximated by $\exp(-i\hat{\omega}_{\text{eff}}T)$ where $\hat{\omega}_{\text{eff}} = \xi\hat{\omega}_A + (1-\xi)\hat{\omega}_B$, using the first-order Taylor expansion. In this case, the effective χ_{ieff} can be obtained as

$$\begin{aligned} \frac{1}{1+\chi_{2\text{eff}}} &= \frac{\xi}{1+\chi_{2A}} + \frac{1-\xi}{1+\chi_{2B}}, \\ \frac{\chi_{1\text{eff}}}{1+\chi_{2\text{eff}}} &= \frac{\xi\chi_{1A}}{1+\chi_{2A}} + \frac{(1-\xi)\chi_{1B}}{1+\chi_{2B}}. \end{aligned} \quad (14)$$

As indicated by the (2,1) entry of $\hat{\omega}$, the nondispersive component $\chi_{2\text{eff}}$ is independently determined by the temporal average of $1/(1+\chi_2)$, denoted as $\langle 1/(1+\chi_2) \rangle$, where “ $\langle \rangle$ ” represents time averaging. In the absence of χ_1 , this aligns with the temporal average of $1/\beta$ for nondispersive systems. For the dispersive component, Eq. (7) remains valid for the temporal averaging of susceptibility $\langle \chi \rangle$ but now has to be normalized by the nondispersive term $(1+\chi_2)$. Specifically, the time-averaged $\langle \chi_1/(1+\chi_2) \rangle$ yields $\chi_{1\text{eff}}/(1+\chi_{2\text{eff}})$, consistent with the (4,1) entry of $\hat{\omega}$. Here, $\chi_{2\text{eff}}$ can be regarded as the background susceptibility (zero in air, assuming no χ_2 contribution). The total effective compressibility then follows $\beta_{\text{eff}} = 1 + \chi_{1\text{eff}} + \chi_{2\text{eff}}$.

Fig. 4 demonstrates the phase transition resulting from modulating the resonant strength a_i while keeping resonant frequency ω_{01} fixed and gradually increasing ω_{02} . The schematic representation is shown in Fig. 4(a). Initially, when both ω_{01} and ω_{02} are small ($\omega_{0i}T \ll 1$), the effective compressibility β_{eff} corresponds to the temporal average of β (equivalent χ), as shown in the left panel of Fig. 4(b). A phase transition occurs when resonant frequency ω_{02} approaches the modulation frequency $1/T = 8\text{kHz}$. As ω_{02} continues to increase, β_{eff} asymptotically converges to the high frequency limit 1.85, as calculated from Eq. (14) (green

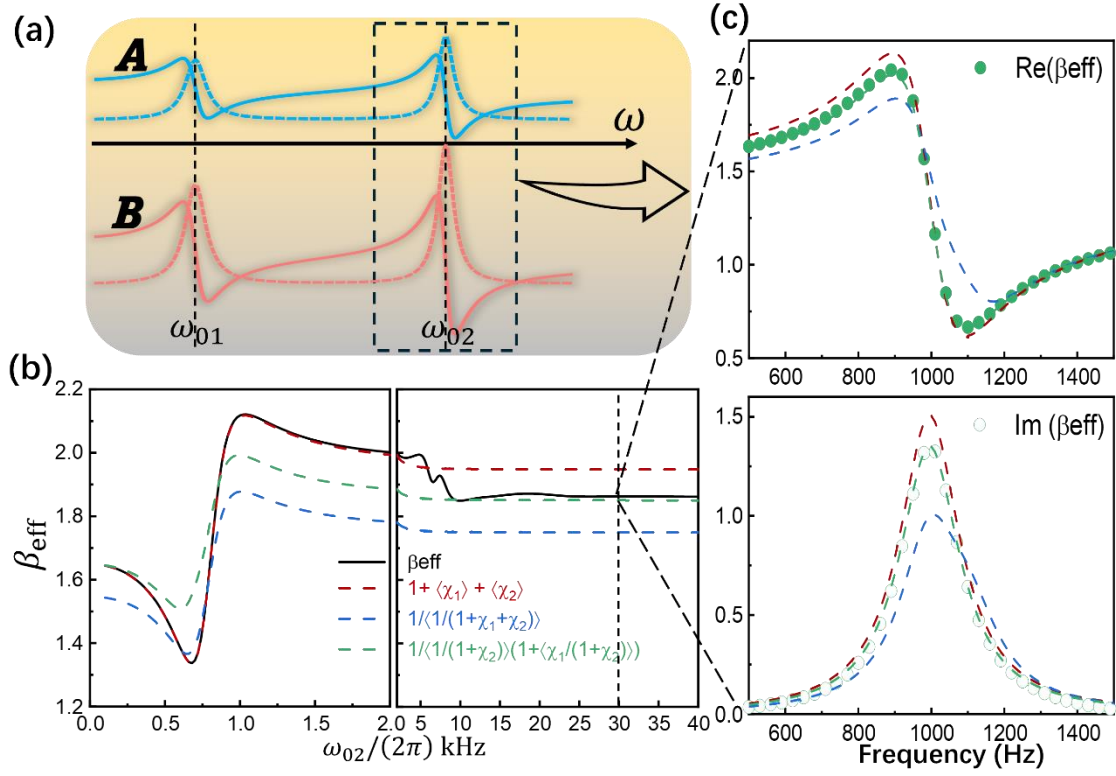


Fig. 4 (a) Conceptual picture of modulating resonant strengths with one resonance (ω_{02}) shifting to high frequencies. (b) Phase transition of a temporal metamaterial with time modulated resonant strengths $a_i(t)$ as ω_{02} increases while fixing $\omega_{01}/(2\pi) = 1\text{kHz}$. The black solid line shows the effective compressibility (β_{eff}) from numerical eigenmode calculations. Red and blue dashed lines represent the temporal average of compressibility (β) and bulk modulus ($1/\beta$), respectively. The green dashed line is the averaging formula from Eq. (14). Resonant strengths alternate between $a_{1A} = 0.1\omega_{01}^2$, $a_{1B} = 0.5\omega_{01}^2$ for $a_1(t)$ and $a_{2A} = 0.1\omega_{02}^2$, $a_{2B} = 0.5\omega_{02}^2$ for $a_2(t)$ with $\xi = 0.5$. The operational frequency and linewidths are $\omega/(2\pi) = 0.8\text{kHz}$, $\gamma_1/\omega_{01} = 0.1$ and $\gamma_2/\omega_{02} = 0.2$. (c) Effective compressibility at varying operational frequencies with modulated resonant strengths $a_i(t)$ at fixed $\omega_{02}/(2\pi) = 30\text{kHz}$ with other parameters in (b). Green solid and hollow dots represent the real and imaginary part obtained from eigenmode approach. The red, green and dashed lines follow the same representations as in (b).

dashed line), shown in the right panel of Fig. 4(b). The effective compressibility β_{eff} obtained from eigenmode approach (black solid lines) agrees with the analytic results for both cases ($\omega_{02}T \ll 1$ and $\omega_{02}T \gg 1$). The operational frequency is fixed at 0.8kHz and detailed parameters used are listed in the caption. To further validate Eq. (14), Fig. 4(c) shows a scan of the operational frequency from 0.5kHz to 1.5kHz , with $\omega_{02}/(2\pi)$ fixed at 30kHz . The eigenmode-extracted effective compressibility (green dots) exhibits excellent agreement with

the analytic predictions (green dashed lines) for both real and imaginary parts, demonstrating the robustness of our temporal effective medium formula across operational frequencies.

Finally, we shift to modulating resonant frequencies ω_{0i} with small ω_{01} ($\omega_{01A/B}T \ll 1$) but large ω_{02} ($\omega_{02A/B}T \gg 1$), as schematically shown in Fig. 5(a). In this case, we adopt the same approach as Eq. (13) to approximate $\hat{\omega}_{\text{eff}}$ but now $\hat{\omega}_A$ and $\hat{\omega}_B$ correspond to resonant frequency pairs $(\omega_{01A}, \omega_{02A})$ and $(\omega_{01B}, \omega_{02B})$, respectively. The effective medium formula can be deduced as:

$$\frac{1}{1 + \chi_{2\text{eff}}} = \frac{\xi}{1 + \chi_{2A}} + \frac{1 - \xi}{1 + \chi_{2B}},$$

$$\frac{1}{\chi_{1\text{eff}}} = \frac{\xi}{\chi_{1A}} + \frac{(1 - \xi)}{\chi_{1B}}.$$
(15)

Similar to the case of modulating resonant strength, the nondispersive part χ_2 , is still governed by the time average of $1/(1 + \chi_2)$. For the dispersive component χ_1 , however, the modulation now affects the resonant frequency, as reflected in the (4,3) entry of $\hat{\omega}$ in Eq.(13). This requires applying Eq. (9) to the temporal average of $1/\chi_1$ to obtain $\chi_{1\text{eff}}$. As an example, we modulate ω_{01} between $\omega_{01A}/(2\pi) = 0.8\text{kHz}$ and $\omega_{01B}/(2\pi) = 1.2\text{kHz}$ and modulate ω_{02} between $\omega_{02A}/(2\pi) = 20\text{kHz}$ and $\omega_{02B}/(2\pi) = 25\text{kHz}$ with duty cycle $\xi = 0.5$. Fig. 5 (a) Schematic of modulating resonant frequencies with $\omega_{01A/B}T \ll 1$ and $\omega_{02A/B}T \gg 1$. Real (b) and imaginary (c) part of effective compressibility of time-varying metamaterial with ω_{01} switching between $\omega_{01A}/(2\pi) = 0.8\text{kHz}$ and $\omega_{01B}/(2\pi) = 1.2\text{kHz}$ and ω_{02} alternating between $\omega_{02A}/(2\pi) = 20\text{kHz}$ and $\omega_{02B}/(2\pi) = 25\text{kHz}$ with duty cycle $\xi = 0.5$. The other parameters are constant: $a_1/(2\pi)^2 = 0.5 \text{ kHz}^2$, $a_2/(2\pi)^2 = 1\text{kHz}^2$, $\gamma_1/(2\pi) = \gamma_2/(2\pi) = 50\text{Hz}$. (b) and (c) show the real and imaginary part of the extracted effective compressibility β_{eff} by eigenmode approach, represented by orange solid and hollow dots. These results agree well with the analytic predictions from Eq. (15), shown as orange dashed line. For comparison, we also plot the time average of β and $1/\beta$ as red and blue lines, both showing up two resonant peaks.

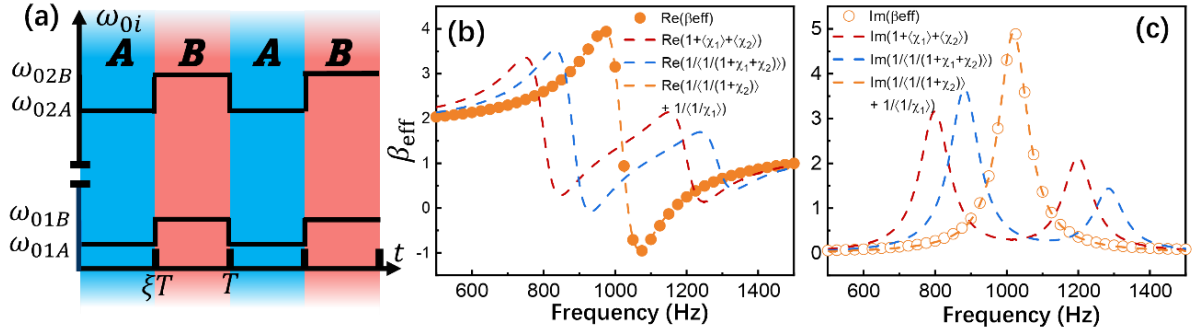


Fig. 5 (a) Schematic of modulating resonant frequencies with $\omega_{01A/B}T \ll 1$ and $\omega_{02A/B}T \gg 1$. Real (b) and imaginary (c) part of effective compressibility of time-varying metamaterial with ω_{01} switching between $\omega_{01A}/(2\pi) = 0.8\text{kHz}$ and $\omega_{01B}/(2\pi) = 1.2\text{kHz}$ and ω_{02} alternating between $\omega_{02A}/(2\pi) = 20\text{kHz}$ and $\omega_{02B}/(2\pi) = 25\text{kHz}$ with duty cycle $\xi = 0.5$. The other parameters are constant: $a_1/(2\pi)^2 = 0.5\text{kHz}^2$, $a_2/(2\pi)^2 = 1\text{kHz}^2$, $\gamma_1/(2\pi) = \gamma_2/(2\pi) = 50\text{Hz}$.

DISCUSSION

In summary, we have established a comprehensive framework for temporal effective medium theory in time-modulated, frequency-dispersive acoustic metamaterials with multiple resonances. Our findings, summarized in Table 1, reveal three key rules governed by the interplay between resonant frequencies (ω_{0i}) and modulation frequency ($1/T$). In the low resonant frequency regime, where both resonant frequencies are much smaller than the modulation frequency ($\omega_{0i}T \ll 1$), the effective compressibility β_{eff} depends on whether the resonant strength a_i or resonant frequency ω_{0i} is modulated: temporal average of monopolar susceptibility χ_i , denoted as $\langle \chi_i \rangle$ for a_i modulation and $\langle 1/\chi_i \rangle$ for modulating ω_{0i} , with β_{eff} emerging as the sum of all contributions of $\chi_{i\text{eff}}$, following $\beta_{\text{eff}} = 1 + \chi_{1\text{eff}} + \chi_{2\text{eff}}$. On the other hand, when both resonant frequencies are large ($\omega_{0i}T \gg 1$), the system falls into the nondispersive regime, giving rise to the temporal average of $1/(1 + \chi_1 + \chi_2)$. Specially, when we have a hybrid case where $\omega_{01}T \ll 1$ and $\omega_{02}T \gg 1$, large ω_{02} will render χ_2 nondispersive, making $1 + \chi_2$ act as a renormalized background. In this case, we first normalize this background via the temporal average of $1/(1 + \chi_2)$, after which the dispersive part χ_1 is treated by either averaging χ_1 but with a scaling factor $1/(1 + \chi_2)$, i.e. $\langle \chi_1/(1 + \chi_2) \rangle$ for modulating resonant strength a_1 or averaging $1/\chi_1$ for modulating resonant

frequency ω_{01} , in accordance with the rule for the low resonant frequency case. Although our analysis focuses on systems with two resonances, the same principles can be extended to acoustic metamaterials with three or more resonances by using the same systematic approach. Beyond acoustics, these findings can be generalized to electromagnetic, elastic, and other classical wave systems, bridging temporal modulation strategies with programmable metamaterial design.

MODULATION PARAMETERS	$\omega_{0i}T \ll 1 (\omega_{0i} \downarrow)$ OR $\omega_{0i}T \gg 1 (\omega_{0i} \uparrow)$	AVERAGE METHOD
a_1, a_2	$\omega_{01} \downarrow, \omega_{02} \downarrow$	$\chi_{1\text{eff}} = \langle \chi_1 \rangle$ $\chi_{2\text{eff}} = \langle \chi_2 \rangle$
a_1, ω_{02}	$\omega_{01} \downarrow, \omega_{02} \downarrow$	$\chi_{1\text{eff}} = \langle \chi_1 \rangle$ $1/\chi_{2\text{eff}} = \langle 1/\chi_2 \rangle$
ω_{01}, ω_{02}	$\omega_{01} \downarrow, \omega_{02} \downarrow$	$1/\chi_{1\text{eff}} = \langle 1/\chi_1 \rangle$ $1/\chi_{2\text{eff}} = \langle 1/\chi_2 \rangle$
a_1, a_2	$\omega_{01} \downarrow, \omega_{02} \uparrow$	$\frac{\chi_{1\text{eff}}}{1 + \chi_{2\text{eff}}} = \langle \frac{\chi_1}{1 + \chi_2} \rangle$ $\frac{1}{1 + \chi_{2\text{eff}}} = \langle \frac{1}{1 + \chi_2} \rangle$
a_1, ω_{02}	$\omega_{01} \downarrow, \omega_{02} \uparrow$	$\frac{\chi_{1\text{eff}}}{1 + \chi_{2\text{eff}}} = \langle \frac{\chi_1}{1 + \chi_2} \rangle$ $\frac{1}{1 + \chi_{2\text{eff}}} = \langle \frac{1}{1 + \chi_2} \rangle$
ω_{01}, a_2	$\omega_{01} \downarrow, \omega_{02} \uparrow$	$1/\chi_{1\text{eff}} = \langle 1/\chi_1 \rangle$ $\frac{1}{1 + \chi_{2\text{eff}}} = \langle \frac{1}{1 + \chi_2} \rangle$
ω_{01}, ω_{02}	$\omega_{01} \downarrow, \omega_{02} \uparrow$	$1/\chi_{1\text{eff}} = \langle 1/\chi_1 \rangle$ $\frac{1}{1 + \chi_{2\text{eff}}} = \langle \frac{1}{1 + \chi_2} \rangle$
a_1, a_2	$\omega_{01} \uparrow, \omega_{02} \uparrow$	$\frac{1}{1 + \chi_{1\text{eff}} + \chi_{2\text{eff}}}$ $= \langle \frac{1}{1 + \chi_1 + \chi_2} \rangle$

Table 1 Summary of effective medium formula for time-modulated acoustic metamaterials with two resonances for different modulation cases: $\beta_{\text{eff}} = 1 + \chi_{1\text{eff}} + \chi_{2\text{eff}}$.

References

- [1] D. R. Smith, W. J. Padilla, D. C. Vier, S. C. Nemat-Nasser & S. Schultz, Composite Medium with Simultaneously Negative Permeability and Permittivity. *Phys. Rev. Lett.* **84**, 4184 (2000).
- [2] Z. Liu. et al. Locally Resonant Sonic Materials. *Science* **289**, 1734 (2000).
- [3] N. Fang. et al. Ultrasonic metamaterials with negative modulus. *Nat. Mater.* **5**, 452 (2006).
- [4] N. Yu. et al. Light Propagation with Phase Discontinuities: Generalized Laws of Reflection and Refraction. *Science* **334**, 333 (2011).
- [5] R. A. Shelby, D. R. Smith & S. Schultz, Experimental Verification of a Negative Index of Refraction. *Science* **292**, 77 (2001).
- [6] J. Valentine. et al. Three-dimensional optical metamaterial with a negative refractive index. *Nature* **455**, 376 (2008).
- [7] J. B. Pendry, Negative Refraction Makes a Perfect Lens. *Phys. Rev. Lett.* **85**, 3966 (2000).
- [8] J. C. Miñano, Perfect imaging in a homogeneous three-dimensional region. *Opt. Express* **14**, 9627 (2006).
- [9] N. Kaina, F. Lemoult, M. Fink & G. Lerosey, Negative refractive index and acoustic superlens from multiple scattering in single negative metamaterials. *Nature* **525**, 77 (2015).
- [10] N. I. Landy, S. Sajuyigbe, J. J. Mock, D. R. Smith & W. J. Padilla, Perfect Metamaterial Absorber. *Phys. Rev. Lett.* **100**, 207402 (2008).
- [11] Y. D. Chong, L. Ge, H. Cao & A. D. Stone, Coherent Perfect Absorbers: Time-Reversed Lasers. *Phys. Rev. Lett.* **105**, 053901 (2010).
- [12] YD. R. Smith & J. B. Pendry, Homogenization of metamaterials by field averaging (invited paper). *J. Opt. Soc. Am. B* **23**, 391 (2006).
- [13] D. Schurig. et al. Metamaterial electromagnetic cloak at microwave frequencies. *Science* **314**, 5801 (2006).
- [14] S. Zhang, C. Xia, & N. Fang, Broadband Acoustic Cloak for Ultrasound Waves. *Phys. Rev. Lett.* **106**, 024301 (2011).

-
- [15] X. Huang, Y. Lai, Z. H. Hang, H. Zheng & C. T. Chan, Dirac cones induced by accidental degeneracy in photonic crystals and zero-refractive-index materials. *Nat. Mater.* **10**, 582 (2011).
 - [16] M. L. N. Chen. et al. Anomalous Electromagnetic Tunneling in Bianisotropic ϵ - μ -Zero Media. *Phys. Rev. Lett.* **129**, 123901 (2022).
 - [17] H. Chen. et al. Design and Experimental Realization of a Broadband Transformation Media Field Rotator at Microwave Frequencies. *Phys. Rev. Lett.* **102**, 183903 (2009).
 - [18] C. Jung. et al. Disordered-nanoparticle-based etalon for ultrafast humidity-responsive colorimetric sensors and anti-counterfeiting displays. *Sci. Adv.* **8**, eabm8598 (2022).
 - [19] X. Wen, H. K. Yip, C. Cho, J. Li & N. Park, Acoustic Amplifying Diode Using Nonreciprocal Willis Coupling. *Phys. Rev. Lett.* **130**, 176101 (2023).
 - [20] C. Caloz & Z. Deck-L  ger, Spacetime Metamaterials—Part I: General Concepts. *IEEE Trans. Antennas Propag.* **68**, 1569 (2020).
 - [21] C. Caloz & Z. L. Deck-L  ger, Spacetime Metamaterials—Part II: Theory and Applications. *IEEE Trans. Antennas Propag.* **68**, 158 (2020).
 - [22] G. Emanuele. et al. Photonics of time-varying media. *Adv. Photonics* **4**, 014002 (2022).
 - [23] H. Moussa. et al. Observation of temporal reflection and broadband frequency translation at photonic time interfaces. *Nat. Phys.* **19**, 863 (2023).
 - [24] E. Lustig. et al. Time-refraction optics with single cycle modulation. *Nanophotonics* **12**, 2221 (2023).
 - [25] T.R. Jones, A.V. Kildishev, M. Segev, & D. Peroulis. Time-reflection of microwaves by a fast optically-controlled time-boundary. *Nat. Commun.* **15**, 6786 (2024).
 - [26] B.L. Kim, C. Chong, & C. Daraio. Temporal Refraction in an Acoustic Phononic Lattice. *Phys. Rev. Lett.* **133**, 077201 (2024).
 - [27] M.-C. Jin, Z.-G. Chen, M.-H. Lu, P. Zhan, & Y.-F. Chen. Temporal uniaxial crystal in a dispersion-modulated lattice model. *Appl. Phys. Lett.* **126**, 041701 (2025).
 - [28] K. Lee. et al. Linear frequency conversion via sudden merging of meta-atoms in time-variant metasurfaces. *Nat. Photon.* **12**, 765 (2018).
 - [29] X. Wen. et al. Unidirectional amplification with acoustic non-Hermitian space–time

-
- varying metamaterial. *Commun. Phys.* **5**, 18 (2022).
- [30] Z.-X. Chen. et al. Robust temporal adiabatic passage with perfect frequency conversion between detuned acoustic cavities. *Nat Commun.* **15**, 1478 (2024).
- [31] T. T. Koutserimpas & R. Fleury. Nonreciprocal Gain in Non-Hermitian Time-Floquet Systems. *Phys. Rev. Lett.* **120**, 087401(2018).
- [32] Y. Wang. et al. Observation of Nonreciprocal Wave Propagation in a Dynamic Phononic Lattice. *Phys. Rev. Lett.* **121**, 194301(2018).
- [33] Z. Chen. et al. Efficient nonreciprocal mode transitions in spatiotemporally modulated acoustic metamaterials. *Sci. Adv.* **7**, eabj1198 (2021).
- [34] X. Guo, H. Lissek & R. Fleury. Observation of non-reciprocal harmonic conversion in real sounds. *Commun. Phys.* **6**, 93 (2023).
- [35] X. Wang. et al. Metasurface-based realization of photonic time crystals. *Sci. Adv.* **9**, eadg7541(2023).
- [36] G. Trainiti. et al. Time-Periodic Stiffness Modulation in Elastic Metamaterials for Selective Wave Filtering: Theory and Experiment. *Phys. Rev. Lett.* **122**, 124301(2019).
- [37] F. Feng, N. Wang & G. P. Wang. Temporal transfer matrix method for Lorentzian dispersive time-varying media. *Appl. Phys. Lett.* **124**, 101701(2024).
- [38] E. Galiffi. et al. Broadband coherent wave control through photonic collisions at time interfaces. *Nat. Phys.* **19**, 1703(2023).
- [39] M. Lyubarov. et al. Amplified emission and lasing in photonic time crystals. *Science*, **377**, 425-428 (2022).
- [40] V. Pacheco-Peña & N. Engheta. Effective medium concept in temporal metamaterials. *Nanophotonics* **9**, 379 (2020).
- [41] P. A. Huidobro, M. G. Silveirinha, E. Galiffi & J. B. Pendry. Homogenization Theory of Space-Time Metamaterials. *Phys. Rev. Appl.* **16**, 014044 (2021).
- [42] P. Garg. et al. Two-step homogenization of spatiotemporal metasurfaces using an eigenmode-based approach. *Opt. Mater. Express* **14**, 549 (2024).
- [43] N. Wang, F. Feng, & G.P. Wang. Nonlocal effective medium theory for phononic temporal metamaterials. *J. Phys.:Condens. Matter.* **36**, 105701 (2024).

-
- [44] Y. Zhai, H.-S. Kwon & B.-I. Popa. Active Willis metamaterials for ultracompact nonreciprocal linear acoustic devices. *Phys. Rev. B* **99**, 220301(R) (2019).
- [45] X. Wen, X. Zhu, H. W. Wu & J. Li. Realizing spatiotemporal effective media for acoustic metamaterials. *Phys. Rev. B* **104**, L060304(2021).
- [46] X. Zhu, H.-W. Wu, Y. Zhuo, Z. Liu & J. Li. Effective medium for time-varying frequency-dispersive acoustic metamaterials. *Phys. Rev. B* **108**, 104303(2023).

Acknowledgements

J.L. acknowledges support from Hong Kong Research Grants Council (RGC) grant (16303019) and AoE/P-502/20.

Author contributions J. Li conceived the idea of time-varying metamaterials with multiple resonances. X. Z. and J. Li set up the theoretical model and the numerical analysis. J. Li and H. W. provided insightful comments on the theoretical explanation. All authors contributed to scientific discussions of the results, explanations and wrote the manuscript.

Competing interests

Authors declare no competing interests.

Data availability

The datasets used and analyzed during the current study are available from the corresponding author upon reasonable request.